


Shock motion inside a varying cross-section channel and consequences on the downstream flow

Florian Hermet ^{*}, Jérémie Gressier , and Nicolas Binder
ISAE-SUPAERO, Université de Toulouse, France



(Received 10 November 2020; accepted 1 April 2021; published 22 April 2021)

Shock wave propagation in a variable cross-section channel is a recurrent issue in the literature. Seminal work regarding this flow configuration has been proposed by Whitham (1958) through the derivation of a one-dimensional approach connecting the shock Mach number and the area channel: the A-M relation. It is based on strong theoretical restrictions: (i) shock equations applied on a C^+ , (ii) omission of the postshock influence, and (iii) initial conditions at rest. It has been the focus of many studies aimed at generalizing it. However, very little attention has been paid to the study of the shock motion outside the varying cross-sectional region since Russell (1967). The objective of the current work is to describe and to explain the shock wave behavior in a constant area channel behind a convergent or divergent channel. It is found that the shock propagation in the downstream uniform area region is influenced by the postshock flow unsteadinesses. Therefore, the Whitham model is not suited to the shock motion study in a constant area region downstream of a convergent or divergent area region. A detailed flow description is provided and a quasisteady model for determining the waves intensity at large times is proposed. This model gives accurate results without any assumptions on the shock strength, area variation or the shock upstream state. Finally, this study points out the limits of the use of Whitham's theory in a variable area channel with increasing section variation rate (where $|dA/A(x + dx)| \geq |dA/A(x)|$).

DOI: [10.1103/PhysRevFluids.6.044802](https://doi.org/10.1103/PhysRevFluids.6.044802)

I. INTRODUCTION

Shock wave propagation in a variable cross-section channel is a recurrent issue in the literature. Many practical occurrences of such an academic configuration exist since it happens in periodic or transient regimes of applications involving compressible gas in ducts. The flow inside a hypervelocity shock tunnel [1] is a typical example, but many others are found in the industry. For example in the field of aeronautical propulsion, recent discussions about the evolution of the turbofan architecture, possibly toward Humphrey's thermodynamic cycle [2], have stimulated the interest of the scientific community concerned by turbomachinery flows for sharp transient regimes. Those would occur as a consequence of an isochoric combustion upstream of the turbines stages, which in turn would be subject to unsteady feeding.

The corresponding prototypical flow consists in the propagation of a shock wave inside a convergent or divergent section, connecting two straight channels of different heights or diameters. The initial state of the compressible fluid can be at rest, or in a steady-state regime. The mention of such a configuration in the literature is found in the seminal works of Chester [3] and Chisnell [4], in which the derivation of the Euler equations reveals the generic behavior expected for the shock wave. The shock Mach number should increase inside a convergent channel (and decrease in a divergent one), which in turn produces an entropy gradient and a complex system of reflected waves. This

*florian.hermet@isae-superaero.fr

has been experimentally confirmed a few years later by Bird [5]. On the modeling ground, the early proposition of Whitham [6] still holds a lot of attention in the scientific community. The theoretical problem is derived through a one-dimensional approach of the shock wave propagation in a gas at rest inside a variable cross-section channel. The entry point of this derivation is the solving of the shock equations along a forward propagating characteristic (C^+). It formalizes the so-called A-M relation, which relates the shock Mach number, M_s , to the local cross-section area of the channel, A . The A-M relation thus predicts the evolution of the shock intensity during its propagation in a convergent or a divergent channel. The first derivation of this relation was restricted to smooth variations of the cross section. An extension for more abrupt geometries is possible, if the effects of the post-shock flow on shock motion are neglected (Whitham [7]).

The A-M relation thus provides a comprehensive modeling of the shock-wave propagation in nonuniform duct flows, widely employed in the literature. Its validity, addressed through a comparison with experimental or numerical data, is questioned in many references: the validity of the Whitham model has been discussed by Igra *et al.* [8] as well as its ability to cope with additional effects such as the influence of the wall shape of the converging [5] or diverging [9,10] channels, or even the maximization of the shock strength [11].

A general consensus of the scientific community is agreed on the fair accuracy of the A-M relation for moderate shock intensity and moderate area ratio, or at least smooth evolution of the convergent channel. The limitations of the model are likely to be a consequence of the strong theoretical restrictions imposed in its the derivation: (i) shock equations applied on a C^+ , (ii) omission of the postshock influence, and (iii) initial conditions at rest. In addition, it appears that a singularity exists at sonic conditions downstream of the shock wave, which has been solved by Friedman [12]. Later, Yousaf [13] and Milton [14] derived an alternative formulation of the A-M relation taking into account the overtaking disturbance on the shock motion, using a set of assumptions. A more general theory emerged a few decades ago and can be found in Best [15]. The author derived a system of differential equations that does not require the omission of the postshock flow effect on the shock motion. The Best model predicts the shock motion at an higher order than the A-M relation. The possibility to prescribe a different initial condition than a quiescent uniform gas is examined by Chisnell [16] and Whitham [17], in which the A-M relation is adapted to the propagation of a shock wave in a moving fluid. Similarly Catherasoo and Sturtevant [18] revised the A-M relation for the case of a nonuniform quiescent gas.

All these studies are focused on the unsteady flow observed inside the convergent or divergent channel. It is indeed in that section that the main interaction between the shock wave and the geometry takes place. However, very little attention has been paid to the shock motion in the straight channel downstream of this critical element. A return to a normal behavior, i.e., a shock wave with a constant intensity, would stand as a reasonable expectation since it propagates in a simple duct. However, this is not the case, and this is seldom mentioned in the literature. The work of Russell [19] seems to be the only one to propose an explicit description of the shock propagation beyond the convergent or divergent section, and it is moreover treated as a side effect. In this experimental study, the author tries to quantify the strengthening of the shock intensity within the convergent channel. For this, pairs of thin-film gauges are used to determine the average speed of the shock wave entering the convergent. Three measurement positions downstream of the convergent channel are also recorded. The shock wave strengthening was actually observed to occur inside the convergent channel, and a progressive decay of the shock intensity was observed in the downstream duct. This decay is briefly analyzed in the work of Russel, and the downstream deceleration was imputed to the viscous dissipation, as well as higher order interactions.

The objective of the present work is to describe and explain the shock wave behavior in an uniform area channel behind a convergent or divergent channel, in an inviscid frame so as to discard viscous effects. Some propositions are made in order to assess the validity of the A-M relation since it is not suitable to predict the shock wave behavior in the downstream straight channel, i.e., at larger time. An accurate description of the flow and the waves interactions during shock wave motion is proposed. A model predicting the flow configuration at larger times is demonstrated to determine

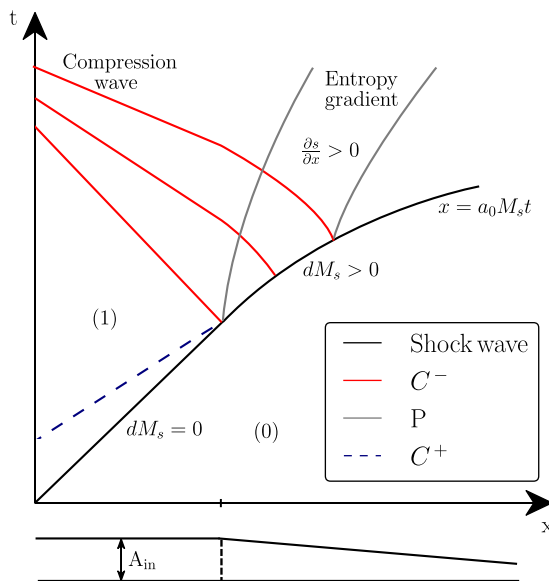


FIG. 1. Spatio-temporal (x,t) diagram for a shock propagating in a convergent duct ($dA < 0$). The flow is subsonic downstream of the shock.

the wave intensities inside the transient flow. The proposed model does not impose any restriction in terms of initial condition of the flow (rest or moving), intensity of the initial shock, or aspect ratio of the convergent/divergent channel.

The paper is organized as follows. In the first section, we briefly review the model of Whitham before discussing its validity in the next section by using numerical simulations. The last part of the paper is dedicated to the description of the long-time flow physics, together with the validation of our model. The paper ends with the conclusions to this study.

II. REVIEW OF WHITHAM MODEL

A. Physics description

We first briefly recall the main flow features when a shock wave propagates through a convergent and/or a divergent channel. We consider a varying cross-section channel in which streamwise evolution is given by

$$\begin{aligned} A &= A_{\text{in}} & \text{if } x < 0 \\ A &= A(x) & \text{if } x > 0. \end{aligned} \quad (1)$$

The flow is initially at rest. A shock wave is imposed initially ($t = 0$) at the inlet of the channel, through the prescription of the inlet boundary conditions. In the first part of the channel (negative values of x), this shock wave propagates in a uniform quiescent gas in a constant section duct. Its propagation speed is constant and measured by the shock Mach number M_s . The flow is thus divided into two uniform regions separated by the shock wave. The undisturbed state ahead of the shock is denoted by (0) while the uniform state prescribed at $t = 0$ behind the shock is denoted by (1).

When the shock reaches the convergent or divergent part of the channel, its intensity is modified in response to the area variation. Therefore, disturbances induced by this modification of the shock intensity travel upstream, following negative characteristic lines (C^-) and the particles paths (P), as illustrated in Fig. 1 for the case of a shock wave propagating through a convergent duct.

The shock wave accelerates, and gains in intensity. Consequently, a reflected compression wave and a positive entropy gradient are generated. On the (x,t) diagram of Fig. 1, the flow behind the shock (1) remains subsonic. For a supersonic downstream flow, the slope of the negative characteristic C^- would be positive. Conversely for a divergent duct, a reflected expansion wave is propagated by the C^- and a negative entropy gradient propagates on the particles path.

As stated in the introduction, the A-M relation gives an accurate prediction of the physics of such a flow configuration. In the next subsection, we recall the theoretical derivation of this model proposed by Whitham [6].

B. Demonstration of the A-M relation

The demonstration proposed by Whitham is based upon the quasi-one-dimensional and inviscid governing equations, written in the characteristic form downstream of the shock:

$$\frac{dp}{\rho a} + du + \frac{ua}{A} \frac{dA(x)}{dx} = 0 \quad \text{for } C^+ : \frac{dx}{dt} = u + a, \quad (2a)$$

$$\frac{dp}{\rho a} - du + \frac{ua}{A} \frac{dA(x)}{dx} = 0 \quad \text{for } C^- : \frac{dx}{dt} = u - a, \quad (2b)$$

$$ds = 0 \quad \text{for } P : \frac{dx}{dt} = u, \quad (2c)$$

where

$$d = \frac{\partial}{\partial t} + \frac{dx}{dt} \frac{\partial}{\partial x} \quad (3)$$

stands for the material derivative; $p = p(M_s)$, $\rho = \rho(M_s)$, $u = u(M_s)$ and $a = a(M_s)$ are the conditions behind the shock, given by the Rankine–Hugoniot jump relationships.

Whitham suggested that the shock path can be approached by that of converging characteristics on the shock. As illustrated in the sketch of Fig. 1, the shock path is approximated by a forward characteristic C^+ . The A-M relation is formalized by the substitution of the differentiated Rankine–Hugoniot jump relations on the differential invariant of the C^+ , Eq. (2a):

$$\frac{1}{A} \frac{dA}{dM_s} = -g(M_s) \quad (4)$$

with

$$g(M_s) = \frac{M_s}{M_s^2 - 1} \left(1 + \frac{2}{\gamma + 1} \frac{1 - \mu^2}{\mu} \right) \left(1 + 2\mu + \frac{1}{M_s^2} \right) \quad (5)$$

$$\mu^2 = \frac{(\gamma - 1)M_s^2 + 2}{2\gamma M_s^2 - (\gamma - 1)}.$$

The validity of this strong assumption made by Whitham to approximate the shock path by a C^+ can be evaluated analytically. Applying the differential invariant of the C^+ to the shock moving at the speed $a_0 M_s$, Whitham claims that Eq. (6) is a good approximation of the shock behavior:

$$\frac{dp}{\rho a} + du + \frac{ua}{A} \frac{dA(x)}{dx} = 0 \quad \text{for } C^+ : \frac{dx}{dt} = a_0 M_s. \quad (6)$$

The difference between Eqs. (2a) and (6) provides a quantification of the error caused by the two assumptions made by Whitham:

$$\frac{1}{u + a} \underbrace{\left(\frac{(u + a) - a_0 M_s}{a_0 M_s} \right)}_1 \underbrace{\left(\frac{\partial p}{\partial t} + \rho a \frac{\partial u}{\partial t} \right)}_2. \quad (7)$$

The first term gives a measure of the coincidence between the shock and the C^+ . For a weak shock, it is close to zero as $a_0 M_s \approx u + a$, however this term tends to 0.274 as $M \rightarrow \infty$ for $\gamma = 1.4$. The second term gives a quantification of unsteadiness in the postshock flow, which modifies the shock strength. It is purely neglected in Whitham's demonstration, and very few comments about it are found in the literature. The discussions are essentially focused on the coincidence between the shock and the C^+ , an assumption that gives to the Whitham approach a better validity for the case of a weak shock rather than for a strong shock. However, the unsteadiness of the postshock flow can induce some errors, even for a weak shock. In the next section, we will show that the postshock unsteadiness must be taken into account to correctly predict the shock intensity downstream of a convergent or divergent duct.

III. VALIDITY OF THE WHITHAM MODEL

According to the A-M relation, the shock motion only depends on both the initial shock strength and the area streamwise variation. A numerical integration of the one-dimensional Euler equations is performed to assess the accuracy of Whitham model. The simulations are carried out thanks to the in-house IC³ solver, borrowed from the CharLES^X solver [20] in which the area variations are modeled by volumic source terms, Eq. (8). IC3 is based on the resolution of the compressible formulation of Euler equations in their conservative form, spatially filtered, on an unstructured mesh using a finite volume method. An explicit third-order Runge-Kutta scheme is used for time advancement while an essentially nonoscillatory second-order shock-capturing scheme is applied to compute flux:

$$\begin{aligned} \frac{\partial \rho}{\partial t} + \frac{\partial \rho u}{\partial x} &= -\frac{\rho u}{A} \frac{dA}{dx} \\ \frac{\partial \rho u}{\partial t} + \frac{\partial (\rho u^2 + p)}{\partial x} &= -\frac{\rho u^2}{A} \frac{dA}{dx} \\ \frac{\partial \rho E}{\partial t} + \frac{\partial (u(\rho E + p))}{\partial x} &= -\frac{u(\rho E + p)}{A} \frac{dA}{dx}. \end{aligned} \quad (8)$$

The shock motion inside a duct with cross-sectional variation is thus considered for different initial strengths and several area variations. The study is performed for a linear convergent channel and restricted to cases for which the flow is subsonic behind the shock. The flow ahead of the shock is at rest, in accordance with Whitham theory.

A. Shock strength prediction inside a variable section channel

Figure 2 shows a comparative study between the prediction given by the A-M relation of Whitham and the results of our numerical simulations. Both weak shock ($\frac{P_1}{P_0} = 1.2$) and a strong shock ($\frac{P_1}{P_0} = 3.0$) configurations are compared for a small ($\frac{A_{in}}{A_{out}} = 1.2$) and a high ($\frac{A_{in}}{A_{out}} = 3.0$) converging ratio.

A good agreement between the theoretical predictions and the numerical simulation can be observed for all cases. As expected, the error increases with the shock strength. The error between simulation and the A-M relation is computed as: $\text{Error} = \left(\frac{P_{\text{simulation}} - P_{\text{A-M}}}{P_{\text{A-M}} - P_0} \right)$, where (0) stands for the undisturbed state ahead of the shock.

The relative error increases with the area ratio. This can be explained by significant flow unsteadinesses. Those postshock flow unsteadinesses are a consequence of the shock strengthening in the converging channel, and can be interpreted as the duct response to the brutal evolution of the flow. The unsteadinesses intensity is stronger when the shock modification is considerable, which happens for large converging ratios. The present results show good agreement with the literature and do not question the accuracy of the A-M relation for these specific flow configurations. However, very few studies have focused on what happens in the straight channel just downstream of the

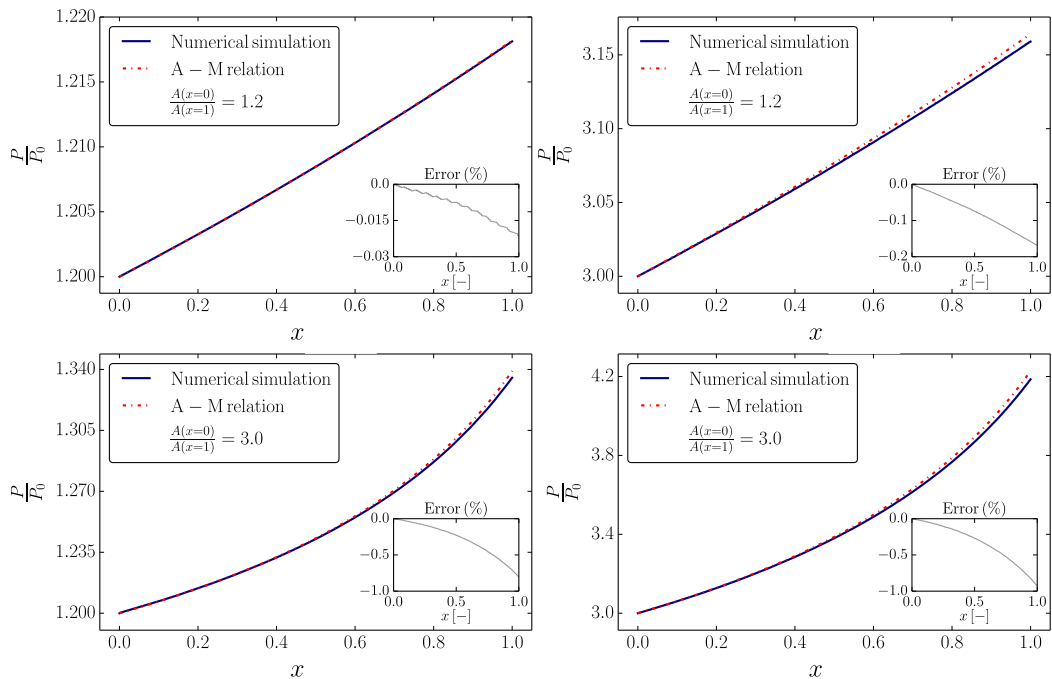


FIG. 2. Comparison between the numerical simulation and the A-M relation for various area ratio and initial shock strength.

convergent/divergent section, in which the A-M relations predicts a constant evolution of the shock. This point is discussed in the following subsection.

B. Shock wave propagating downstream of the convergent channel

The shock motion is investigated for a single initial pressure ratio ($\frac{P_1}{P_0} = 1.2$) and single convergent channel linear ratio ($\frac{A_{in}}{A_{out}} = 3$), but now the region of interest is extended to the constant area channel following the convergent section.

Figure 3(a) presents the evolution of the shock pressure ratio along its propagation inside the channel, predicted by the numerical simulation and the A-M relation. It is clear that the shock strength does not remain constant in the straight channel downstream of the convergent channel, as predicted by the A-M relation. The shock wave intensity actually decreases, since it is weakened by a forward propagating expansion wave. This expansion wave comes from the interaction between the backward propagating compression wave (the reflected wave), the entropy gradient created by the shock strengthening inside the convergent duct and convected by the flow, and the cross-section evolution. Since the backward traveling reflected wave is a compression wave that evolves in a divergent section (because of the backward direction), an expansion wave is created, this time traveling in the flow direction. All these effects compose the complex and unsteady postshock flow that activates term 2 in Eq. (7).

However, it may be surprising at first sight that the postshock flow effects have more influence on the shock motion in the downstream straight channel, rather than in the convergent/divergent section. Actually, it is not as explained by Best [15].

Best demonstrated a valid recurrence relation along the shock path predicting the shock-wave intensity. This relation is a handling of the Euler equations, which does not require any of the

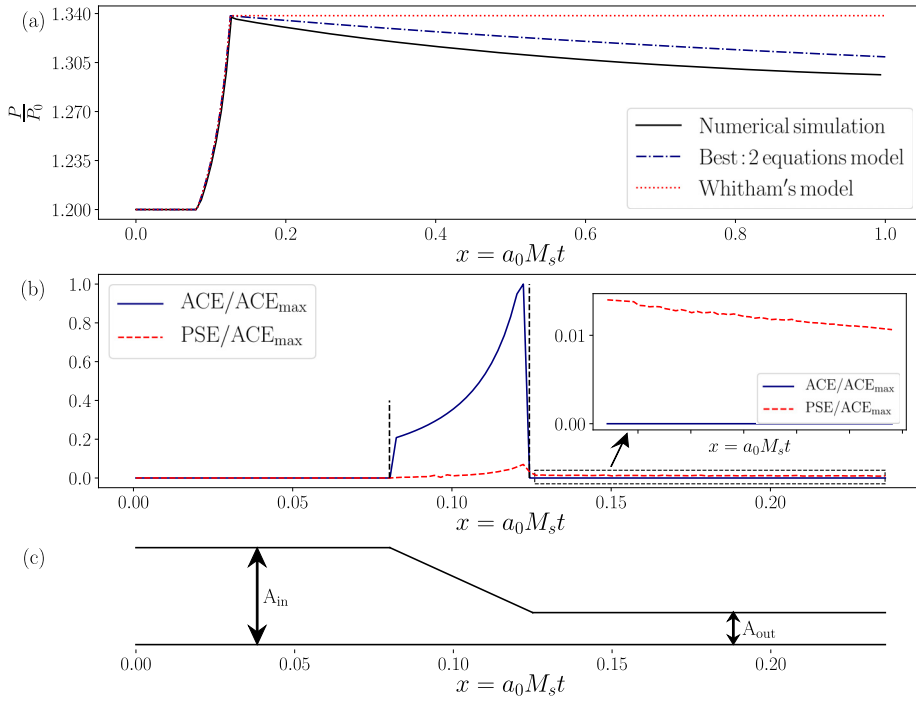


FIG. 3. (a) Shock strength comparison between the numerical simulation, the Whitham model and the Best's model. (b) Investigation of the area change (ACE) and of the postshock flow unsteadiness (PSE) terms on the shock strength. (c) Area evolution.

forementioned assumptions used by Whitham; for more details see Best [15]. The final equations of Best model are

$$dM_s = \frac{-a_0 M_s}{dM_s p + \rho a dM_s u} \left[\left(\frac{\rho a^2 u}{u+a} \right) \frac{1}{A} \frac{dA}{dx} + \left(\frac{1}{u+a} - \frac{1}{a_0 M_s} \right) Q_1 \right], \quad (9a)$$

$$\forall k \geq 1, \quad dQ_k = -a_0 M_s \left[\frac{\partial^k}{\partial t^k} \left(\frac{\rho a^2 u}{u+a} \right) \frac{1}{A} \frac{dA}{dx} + \sum_{i=1}^k \binom{k}{i} \frac{\partial^i}{\partial t^i} \left(\frac{1}{u+a} \right) Q_{k-i+1} \right. \\ \left. + \frac{\partial^{k-1}}{\partial t^{k-1}} \left(\frac{\partial \rho a}{\partial t} \frac{\partial u}{\partial x} - \frac{\partial \rho a}{\partial x} \frac{\partial u}{\partial t} \right) \right] - \left(\frac{a_0 M_s}{u+a} - 1 \right) Q_{k+1} \quad (9b)$$

with

$$d = \frac{\partial}{\partial t} + a_0 M_s \frac{\partial}{\partial x} \\ Q_{k+1} = \frac{\partial^k}{\partial t^k} \left(\frac{\partial p}{\partial t} + \rho a \frac{\partial u}{\partial t} \right), \quad \forall k \geq 0 \quad (10)$$

$dM_s p$ (resp. u) represents a derivative of $p(M_s)$
(resp. $u(M_s)$) to M_s ,

and show that the truncation of Best's recurrence system to the first equation (i.e., $Q_1 = 0$ and consequently $dQ_k = 0$) allows us to get back exactly the A-M relation proposed by Whitham.

Thus, a reliability criterion of the A-M relation can be given, based on Eq. (9a):

$$\underbrace{a_0 M_s \frac{\rho a^2 u}{u+a} \left| \frac{1}{A} \frac{dA}{dx} \right|}_{\text{ACE}} \gg \underbrace{\left| \frac{a_0 M_s}{u+a} - 1 \right| \left| \frac{\partial p}{\partial t} + \rho a \frac{\partial u}{\partial t} \right|}_{\text{PSE}}. \quad (11)$$

The left-hand side of Eq. (11) depicts the area change effects (ACE) on the shock strength. The right-hand side has already been described in the previous section as the error carried out by the A-M relation, and corresponds to the post shock effects (PSE). From equation (11), it is clear that the Whitham model is accurate when the area change effects are predominant over the shock propagation, compared to the post-shock flow effects.

The post-processing of the numerical simulations gives access to the exact balance between the two physical mechanisms: the ACE and the unsteady PSE. Figure 3(b) shows the evolution of each of the two terms, immediately behind the shock; following its propagation. Obviously, $\text{ACE} = 0$ for each straight part of the channel, which actually makes those regions very sensitive to postshock effects. In the first straight part of the channel, the shock propagation is uniform, which makes $\text{PSE} = 0$ and, as a consequence, the Whitham model is exact. In the converging section PSE is activated, but so is ACE, which is one or even two orders of magnitude higher than PSE: the error of the model exists but it is not perceptible. Consequently, Whitham theory fits very well the simulations in that part of the channel. Then, in the downstream straight section, PSE is still activated because of the expansion wave traveling upstream, but $\text{ACE} = 0$: the error gets significant and the Whitham model is inaccurate. Finally, effects due to the postshock flow disturbances tend towards zero as the shock strength converges to its asymptotic value in the uniform channel.

The truncation at the second equation of Best system is also examined in Fig. 3. In the converging section, no real improvement is to be expected. In the downstream straight channel, a decay of the shock intensity is effectively predicted, since the postshock effects are partially computed. But the truncation makes the prediction at long time (i.e., when the interaction between the shock and the expansion wave is over) quite inaccurate, compared with the direct simulation. A higher order truncation or a closure model would allow getting a more pertinent strength at long time by better modeling the postshock unsteadinesses [Eq. (9a)]. However, the recurrence system demonstrated by Best [Eq. (9)] is quite complex to solve at a higher order: to the authors knowledge, no implementation of Best model with $k \geq 2$ or with a closure model has ever been carried out.

For completeness, it must be stated that some models of the literature, such as found in Yousaf [13] and Milton [14], also include the postshock flow effects on the shock motion, but this modeling is only active in the converging/diverging section (when $dA = 0$ the shock strength no longer varies in their modeling). This is unfortunate since no correction of the Whitham model is needed in that region, as opposed to the downstream constant section channel of this region for which the postshock flow effects should be taken into account in order to capture the shock decay.

C. Nonlinear area variation in the converging/diverging section

In the previous simulations, $A(x)$ is linear. This provokes a brutal cancellation of the ACE term at the inlet of the straight channel, which might not be representative of more realistic cases, where the geometric interface might be more progressive. Some cases for which dA varies in the converging section are examined in that purpose. The initial strength of the shock and the global area variation are the same as previously: $\left(\frac{P_1}{P_0} = 1.2\right)$ and $\left(\frac{A_{\text{in}}}{A_{\text{out}}} = 3.0\right)$.

Figure 4 shows the influence of the sign of d^2A on the intensity of the ACE term. Actually, the result observed does not drastically change the former conclusions: the error gets significant when the condition given by Eq. (11) is no more respected. Anyway, it moderates the assessment that the Whitham model is valid inside the converging section since, technically, this condition is violated while the shock wave is still inside the convergent channel. A strong correlation is found between the variation of the ACE and that of d^2A . However, a generic criterion based on the geometry variation

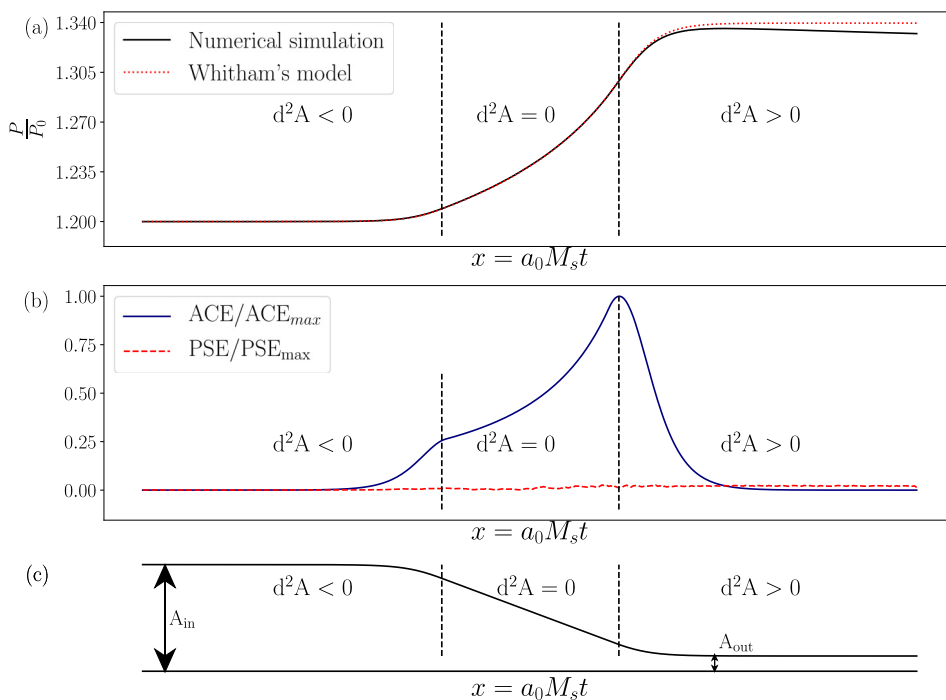


FIG. 4. Investigation of the d^2A variation through the non-uniform region. (a) shock strength during its propagation. (b) terms of Eq. (11), each term is normalized by the maximum of ACE. (c) the area evolution along the geometry.

seems out of the reach of analytical derivation. But it could be guessed that the Whitham model gives relatively accurate results when $|dA(x + dx)| \geq |dA(x)|$ and cannot provide good results when $|dA(x + dx)| < |dA(x)|$. Unfortunately, the condition $|dA(x + dx)| \geq |dA(x)|$ never holds at the end of the convergent/divergent duct, where the channel becomes straight, no matter how smoothly. A specific model is thus required to predict the decay of the shock wave, caused by PSE term. Such a long-time model is proposed in the following section.

IV. PHYSICS DESCRIPTION

The physical framework of the model is recalled, illustrated by the specific case of a shock wave propagating inside a linear convergent channel followed by a straight channel; the flow downstream the shock is still considered as subsonic. But this focus on a given configuration does not alter the generic nature of the model, as will be shown in the following sections.

The physical description proposed in Sec. III B is illustrated in the (x, t) diagram of Fig. 5. The key features are briefly summarized:

- (1) the shock strengthens in a convergent (respectively, weakens in a divergent) channel due to the cross-section change;
- (2) a compression wave is reflected (respectively, an expansion wave for $dA < 0$) in the post-shock flow, traveling at $u - a$;
- (3) an entropy gradient is created by the varying shock intensity, traveling at postshock flow speed u ;

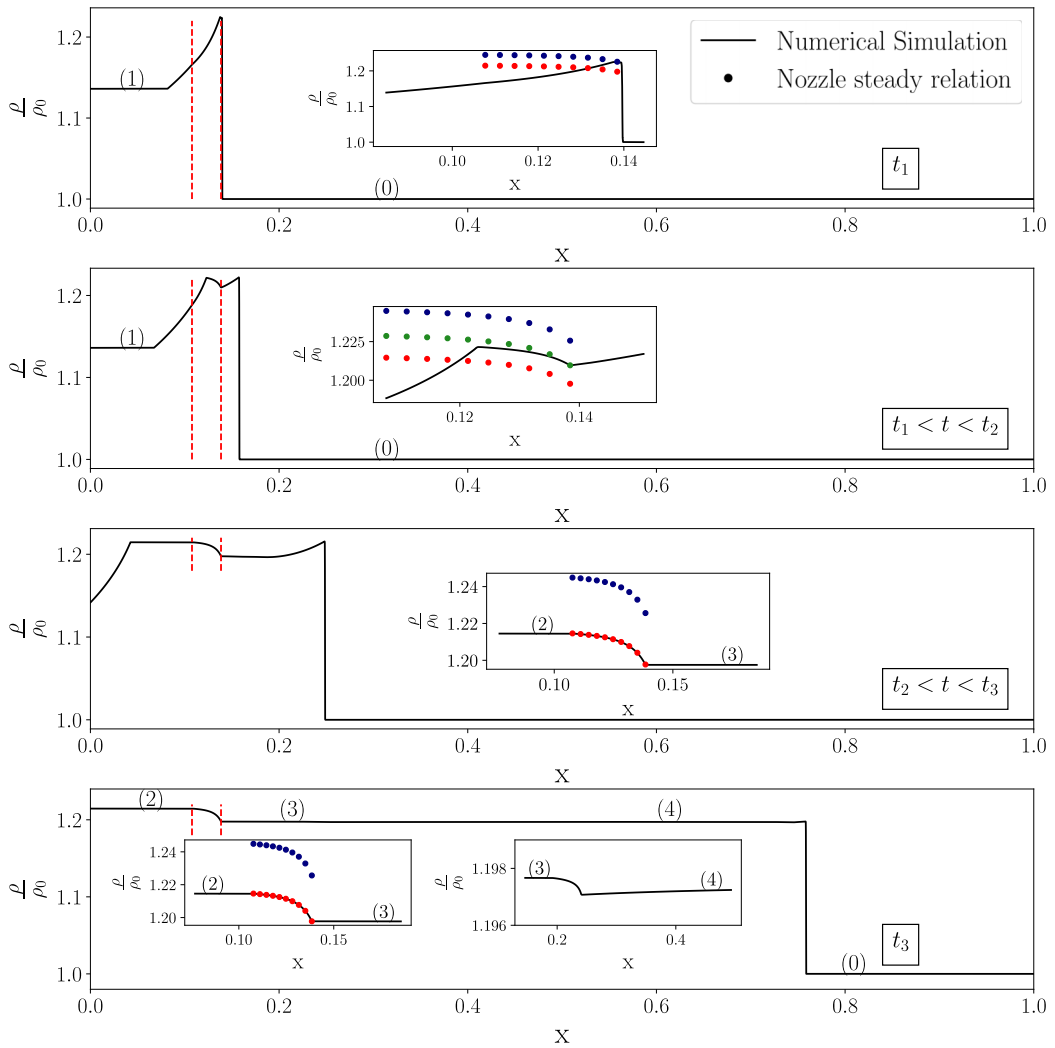


FIG. 6. Density is plotted for the specified times on Fig. 5. $\frac{P_1}{P_0} = 1.2$, $\frac{A_{in}}{A_{out}} = 3.0$. Red, green, and blue circles are, respectively, the nozzle steady relation computed from the final steady state, instantaneous states and the state just behind the shock wave, in the outlet cross section of the convergent channel.

Fig. 5, corresponds to the position of the shock wave exactly at the outlet of the converging section. The state of the gas inside the convergent duct is not compatible with the quasisteady approach, and the same is true for a moment before t_2 . At t_2 , which corresponds to an instant following the departure of the last C^+ of the streamwise expansion wave from the convergent channel, the flow is adapted to the quasisteady solution.

The complete attenuation of the wave interactions inside the convergent channel, together with a stabilization of the shock wave intensity, marks the beginning of the long time state (t_3 , in Figs. 5 and 6). At long time, states (2), (3) and (4) (Fig. 5) persist in the flow (Fig. 6), until a possible wave interaction with the boundaries of the straight channel. The next section is dedicated to the determination of these states.

V. ESTABLISHED FLOW MODEL

A. Model description

The model is based on the aforementioned observation: the flow in the convergent/divergent section can be approximated by the quasisteady approach as soon as the streamwise expansion leaves this section. The validity should thus be restricted to area ratios lower than 10, but the following section will show that it provides fair prediction even above that limit.

The states (1) and (2) are separated by an isentropic compression wave (Fig. 5) in a straight section, so the Riemann invariant along a C^+ characteristic for a perfect gas together with the isentropic relation gives

$$\begin{aligned} u_1 + \frac{2a_1}{\gamma - 1} &= u_2 + \frac{2a_2}{\gamma - 1} \\ \frac{P_1}{a_1^{\frac{2\gamma}{\gamma-1}}} &= \frac{P_2}{a_2^{\frac{2\gamma}{\gamma-1}}}. \end{aligned} \quad (12)$$

The flow inside the convergent channel is here considered as quasisteady, as formerly stated. Therefore, the classical steady relations of mass flow and entropy conservation can be applied between states (2) and (3), where P_i represents the stagnation pressure:

$$\begin{aligned} \frac{A_{\text{in}}}{A_{\text{out}}} &= \frac{M_3 \left(1 + \frac{\gamma-1}{2} M_2^2\right)^{\frac{\gamma+1}{2(\gamma-1)}}}{M_2 \left(1 + \frac{\gamma-1}{2} M_3^2\right)^{\frac{\gamma+1}{2(\gamma-1)}}} \\ P_3 &= P_{i_2} \left(1 + \frac{\gamma-1}{2} M_3^2\right)^{-\frac{1}{\gamma-1}} \\ \frac{P_2}{a_2^{\frac{2\gamma}{\gamma-1}}} &= \frac{P_3}{a_3^{\frac{2\gamma}{\gamma-1}}}. \end{aligned} \quad (13)$$

States (3) and (4) are only separated by an entropy gradient. On each side of this gradient, conditions are the same as those of a contact discontinuity, hence:

$$P_4 = P_3 \quad \text{and} \quad u_4 = u_3. \quad (14)$$

Thanks to the Rankine–Hugoniot equations, which can be applied between states (0) and (4), state (4) is determined by shock intensity or velocity.

The right number of relations has been obtained to close the problem and determine states (2), (3), and (4). Thus, all long-time states can be determined through an iterative process:

(1) initialization of the reflected wave intensity between (1) and (2), state (2) is then fully determined;

(2) nozzle steady relations provide state (3);

(3) contact discontinuity relations enforce velocity and pressure of state (4);

(4) shock intensity is then determined to match the pressure condition of state (4) through Rankine–Hugoniot relations, which also prescribe the entropy gradient and the velocity;

(5) the postshock velocity of state (4) must match the already prescribed velocity; otherwise, the initial guess for the reflected wave strength is wrong and must be modified accordingly until convergence.

No assumptions about the shock initial strength, the cross-sectional variation intensity or the upstream state to the shock are required. Furthermore, the maximum value of entropy in the flow, between the positive and negative entropy gradients, can be estimated using the A-M relation or Best model for a quiescent gas ahead of the shock. For a moving flow, it can be estimated with Chisnell's model [16].

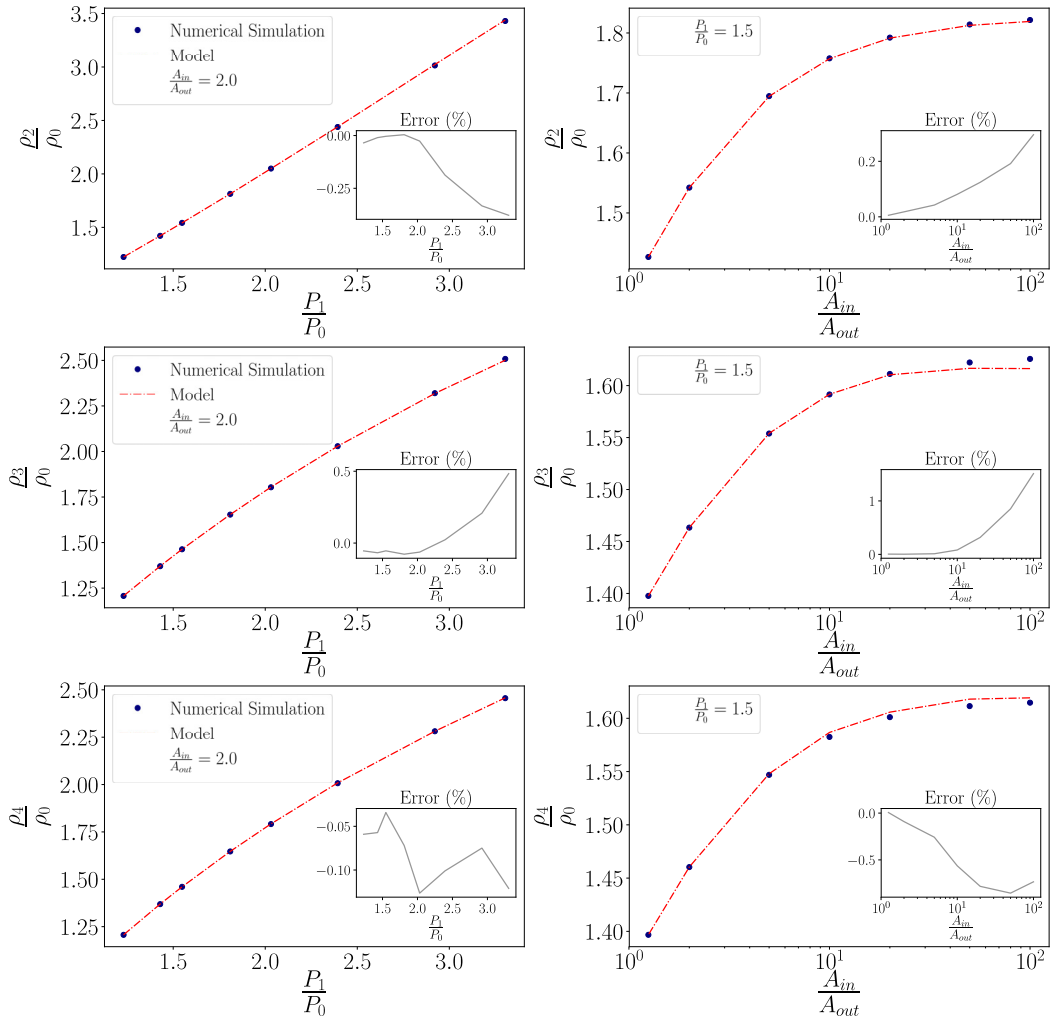


FIG. 7. Comparison between numerical simulation and long time model for different initial shock strength and for various linear area change.

B. Model validation

In order to validate the model, comparisons with numerical simulations are performed inside a linear convergent channel located between two straight sections, for several initial shock intensities. Comparisons are achieved by examining the density, since this quantity varies across states (2), (3) and (4) (Fig. 5) unlike the pressure or velocity, for which a continuity is expected across the entropy gradient.

For a fixed area ratio and several initial shock strengths (graphs on the left in Fig. 7), the model gives very good results. The long-time transmitted shock wave is very well predicted since the error is less than 1%. There is no clear trend regarding the evolution of the error between the numerical simulation and the model: the transmitted shock wave or reflected wave are accurately predicted for an initial strong shock as well as for a weak shock. The error is performed as $\text{Error} = \left(\frac{\rho_{\text{model}} - \rho_{\text{simulation}}}{\rho_{\text{simulation}} - \rho_0} \right)$.

The model shows also excellent results for a range of converging ratio at constant initial shock intensity (graphs on the right in Fig. 7). However, the error tends to increase for large ratio, as

expected above 10. However, even for large cross-sectional variations, the results are acceptable (Errors <2%).

The validation presented here is restricted to a linear variation inside a convergent duct, for compactness. However, similar results have been obtained for non-linear section variations, and for divergent sections. Indeed, no hypothesis is required on the section variation shape in Eq. (13). And even if the physics actually change for a divergent (the reflected compression wave is replaced by a reflected expansion wave), it has no consequences regarding the model since the equations through an isentropic compression or an isentropic expansion wave remain the same. Therefore, the model still holds.

VI. CONCLUSION

This paper highlights the physics of the flow created by the shock wave propagation through a variable area channel. Current models are assessed by resolved numerical simulations and their limitations are demonstrated, more specifically in the straight section downstream of a converging (or diverging) region. This paper demonstrates that the shock-wave strength can be drastically modified by the postshock flow unsteadinesses, which contrasts with Whitham's assumptions in the derivation of the well-known A-M relation. The mechanism of interaction between the reflected waves, which provoke this postshock unsteadiness, and the shock wave itself is described in the paper, and illustrated by the use of (x,t) diagrams. Its influence on the shock-wave intensity is hardly perceptible inside the converging/diverging section, which makes the Whitham model quite valid in that region. But it strongly increases in the downstream straight channel, and prevents any accurate prediction at long time with existing models of the literature, including the Best model with two equations. A higher truncation of the Best model would probably enhance its accuracy, but the cost of resolution becomes comparable to that of a direct simulation.

A simple quasisteady model is also proposed in this paper. This model accurately predicts the long time waves intensity, without any hypothesis on initial shock wave strength or regarding the area variation intensity, as well as on the shock upstream flow state (rest or moving). The validity of the model is assessed on the specific case of a linearly converging section in this paper, but it has been observed with equal accuracy for nonlinear evolution of the area and/or diverging sections.

ACKNOWLEDGMENTS

The authors thank the DGA for their financial support and for permitting the publication of the research. This work was performed using HPC resources from GENCI-IDRIS and GENCI-CINES on Jean-Zay, Occigen (Grant No. 2020-A0102A07178) and CALMIP on Olympe (Grant No. 2020-p1425).

-
- [1] O. Igra, L. Wang, J. Falcovitz, and O. Amann, Simulation of the starting flow in a wedge-like nozzle, *Shock Waves* **8**, 235 (1998).
 - [2] G. D. Roy, S. M. Frolov, A. A. Borisov, and D. W. Netzer, Pulse detonation propulsion: challenges, current status, and future perspective, *Prog. Energy Combust. Sci.* **30**, 545 (2004).
 - [3] W. Chester, CXLV. The quasi-cylindrical shock tube, *London Edinburgh Philos. Mag. J. Sci. London* **45**, 1293 (1954).
 - [4] R. F. Chisnell, The normal notion of a shock wave through a non-uniform one-dimensional medium, *Proc. R. Soc. London A* **232**, 350 (1955).
 - [5] G. A. Bird, The effect of wall shape on the degree of reinforcement of a shock wave moving into a converging channel, *J. Fluid Mech.* **5**, 60 (1959).
 - [6] G. B. Whitham, On the propagation of shock waves through regions of non-uniform area or flow, *J. Fluid Mech.* **4**, 337 (1958).

- [7] G. B. Whitham, *Linear and Nonlinear Waves*, Pure and Applied Mathematics: A Wiley Series of Texts, Monographs and Tracts (Wiley, New York, 1974).
- [8] O. Igra, T. Elperin, J. Falcovitz, and B. Zmiri, Shock wave interaction with area changes in ducts, [Shock Waves](#) **3**, 233 (1994).
- [9] M. A. Nettleton, Shock attenuation in a gradual area expansion, [J. Fluid Mech.](#) **60**, 209 (1973).
- [10] J. J. Gottlieb and O. Igra, Interaction of rarefaction waves with area reductions in ducts, [J. Fluid Mech.](#) **137**, 285 (1983).
- [11] J. Dowse and B. Skews, Area change effects on shock wave propagation, [Shock Waves](#) **24**, 365 (2014).
- [12] M. P. Friedman, An improved perturbation theory for shock waves propagating through non-uniform regions, [J. Fluid Mech.](#) **8**, 193 (1960).
- [13] M. Yousaf, The effect of overtaking disturbances on the motion of converging shock waves, [J. Fluid Mech.](#) **66**, 577 (1974).
- [14] B. Milton, Mach reflection using ray-shock theory, [AIAA J.](#) **13**, 1531 (1975).
- [15] J. P. Best, A generalisation of the theory of geometrical shock dynamics, [Shock Waves](#) **1**, 251 (1991).
- [16] R. F. Chisnell, A note on Whitham's rule, [J. Fluid Mech.](#) **22**, 103 (1965).
- [17] G. B. Whitham, A note on shock dynamics relative to a moving frame, [J. Fluid Mech.](#) **31**, 449 (1968).
- [18] C. J. Catherasoo and B. Sturtevant, Shock dynamics in non-uniform media, [J. Fluid Mech.](#) **127**, 539 (1983).
- [19] D. A. Russell, Shock-wave strengthening by area convergence, [J. Fluid Mech.](#) **27**, 305 (1967).
- [20] G. A. Bres, F. E. Ham, J. W. Nichols, and S. K. Lele, Unstructured large-eddy simulations of supersonic jets, [AIAA J.](#) **55**, 1164 (2017).
- [21] R. Courant and K. O. Friedrichs, *Supersonic Flow and Shock Waves* (Springer-Verlag, New York, 1967).
- [22] G. De Laval, Steam turbine (1894), U.S. Patent 522,066 A.